

## Electronic Supporting Information (ESI)

### Structural Basis for Two-Dimensional Flexible Pharmaceutical Solvate Crystal: Indomethacin Methanol

Aritra Bhowmik,<sup>a</sup> Sanjivani Bamane,<sup>a</sup> and Manish Kumar Mishra<sup>a,b,\*</sup>

<sup>a</sup>Physical and Materials Chemistry Division, CSIR-National Chemical Laboratory, Dr. Homi Bhabha Road, Pashan, Pune, 411008 India.

<sup>b</sup>Academy of Scientific and Innovative Research (AcSIR), Sector 19, Kamla Nehru Nagar, Ghaziabad, Uttar Pradesh 201002, India.

Email addresses: [mk.mishra@ncl.res.in](mailto:mk.mishra@ncl.res.in) and [mishra\\_mani07@yahoo.in](mailto:mishra_mani07@yahoo.in)

#### List of contents:

**S1. Experimental details**

**S2. Single crystal X-ray diffraction experiment**

**S3. Face indexing of INDM crystal**

**S4. Intermolecular interactions and interlocked packing**

**S5. Three-point bending of INDM crystal**

**S6. Energy framework calculations**

**S7. Raman Spectra of elastic INDM**

**S8. Calculated Raman spectra of INDM**

**S9. SC-XRD frames before and after bending of INDM crystal**

**Video S1. Three-point bending of (10-1/-101) face (MP4)**

**Video S2. Three-point bending of (101/-10-1) face (MP4)**

**Video S3. Looping test of (10-1/-101) face (MP4)**

#### Abbreviation:

**INDM:** Indomethacin Methanol solvate

## S1. Experimental Details

**Materials:** Indomethacin was purchased from TCI Pvt. Ltd. (Tokyo Chemical Industry India Pvt. Ltd.) and the solvent Methanol was purchased from Finar Chemicals Pvt. Ltd. and used as received.

**Single crystal preparation of elastic crystal of INDM:** 100 mg of as-received Indomethacin was dissolved in 5mL of methanol (MeOH) and left to slowly evaporate. After 4 to 6 days, long thin needle-like crystals formed from the solution. These needle crystals were utilized for single-crystal X-ray diffraction (SCXRD) and bending experiments. Following the SCXRD analysis, it was established that the crystals were **Indomethacin Methanol solvate (INDM)**.

## S2. Single Crystal X-ray Diffraction Experiment

Good-quality single crystals of INDM suitable for single-crystal X-ray diffraction experiment were selected using a Leica polarizing microscope (S8 APO). Single crystal X-ray diffraction (SCXRD) of INDM was performed on a Bruker D8 VENTURE Kappa Duo PHOTON II CPAD diffractometer equipped with a Mo micro-focus sealed X-ray tube [ $\lambda$  (Mo  $K\alpha$ ) = 0.71073 Å, generator power 50 kV and 1.4 mA] and Incoatech multilayer mirror optics. The crystals of INDM were confirmed by checking and comparing the cell parameters with the reported crystal structure BANMUZ.<sup>1</sup> (see Table S1).

**Table S1. Crystallographic information table for INDM:**

CCDC Refcode	<b>BANMUZ</b>
Empirical formula	$C_{20}H_{20}ClNO_5$
Molecular weight	389.82
Crystal system	Monoclinic
Space group	$P2_1/n$
$a$ (Å)	18.073(2)
$b$ (Å)	5.029(1)
$c$ (Å)	20.901(2)
$\alpha$ (°)	90
$\beta$ (°)	100.74 (1)
$\gamma$ (°)	90
Volume, $V$ (Å <sup>3</sup> )	1866.347
$Z/Z'$	4/1

### S3. Face Indexing of INDM Crystal

Face indexing of needle shaped INDM crystal was done by Bruker D8 Venture, Kappa Duo PHOTON II CPAD diffractometer with a Mo micro-focus sealed X-ray tube [ $\lambda$  (Mo  $K\alpha$ ) = 0.71073 Å, generator power 50 kV and 1.4 mA] and Incoatech multilayer mirror optics. Here we identified the major face is (10-1)/(-101), minor face is (101)/(-10-1) and the end face is (010)/(0-10).

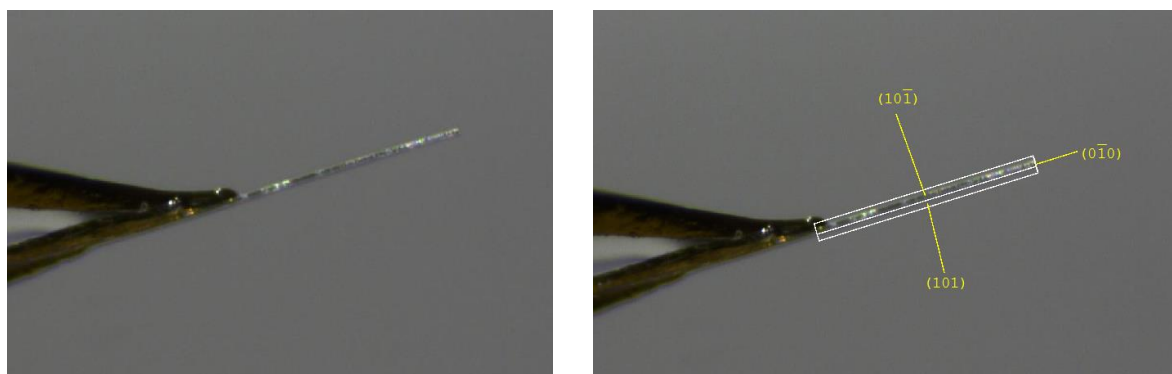


**Figure S1.** (Left) Crystal before face indexing. (Right) Face indexed crystal shows different faces of needle shaped INDM crystal.

### S4. Intermolecular Interactions and Interlocked Packing

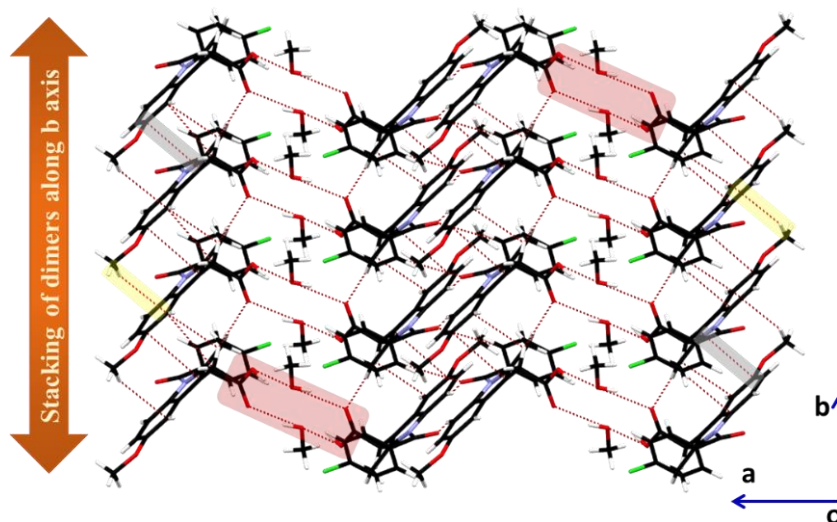


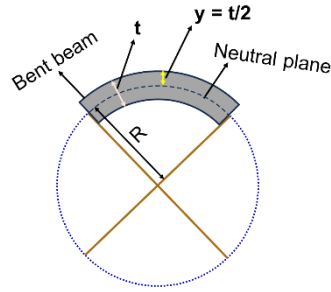
**Figure S2.** Stacking of dimers along *b*-axis and interlocked layered structure of INDM molecule, with C-H $\cdots$  $\pi$  (yellow),  $\pi\cdots\pi$  (grey) and O-H $\cdots$ O dimer (red) interactions.

### S5. Three-point Bending Test of INDM Crystals.

The metallic needle and forceps were used to conduct the three-point bending and looping tests on the major (10-1/-101) and minor (101/-10-1) faces of elastic INDM needle-shaped crystals. The Polarized Light Microscope (Leica polarizing microscope (S8 APO) was utilized to record the test video on the screen. The ImageJ program<sup>2</sup> was employed to measure the thickness and radius of the bent INDM crystal.

#### Calculation of bending strain:

The Euler-Bernoulli beam theory<sup>3</sup> is employed to calculate the strain during the elastic bending of a beam when the deflection is purely due to bending and does not include any shear component.



$$\varepsilon_x = \frac{y}{R} \times 100\% \quad (1)$$

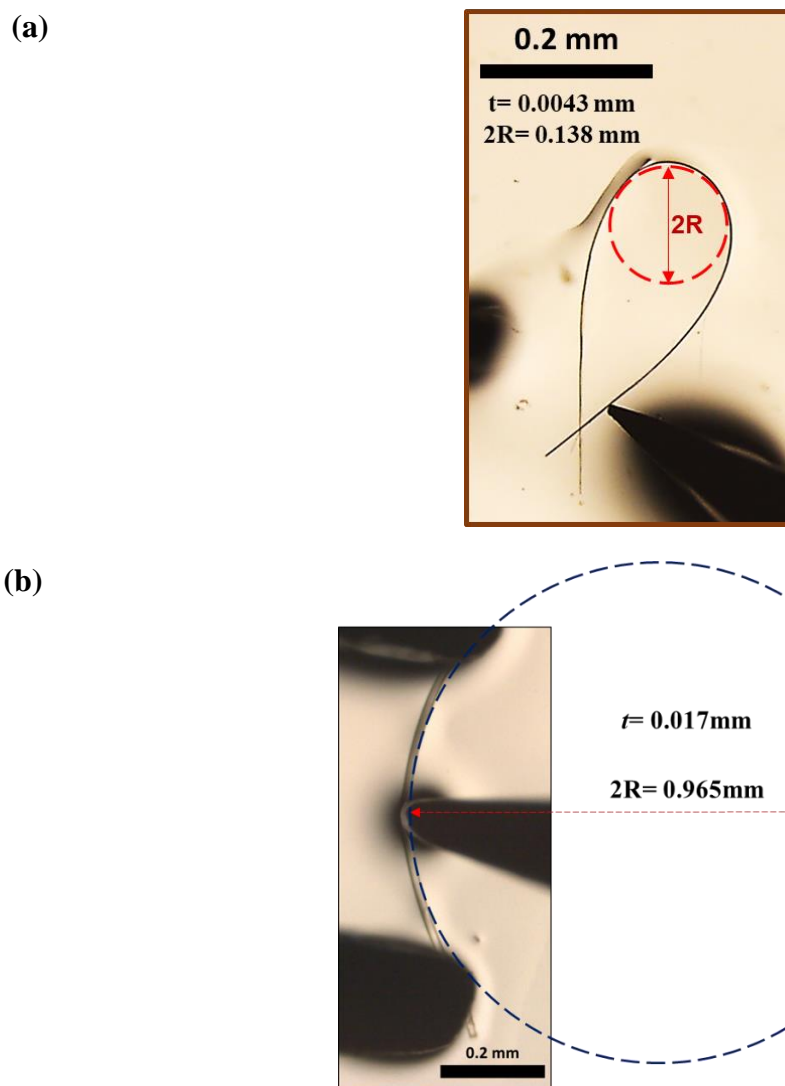
In this context,  $\varepsilon_x$  represents the normal strain,  $y$  denotes the distance from the plane of interest to the neutral plane (which remains constant in length and position during bending), and  $R$  represents the radius of curvature of the neutral plane. If we denote the measured thickness of a crystal as  $t$  and the measured radius,  $R$ , of curvature of the bent crystal, the absolute value of  $\varepsilon_x$  can be expressed as follows:

$$\varepsilon_x = \frac{t/2}{R} \times 100\% \quad (2)$$

$$\varepsilon_x = \frac{t}{2R} \times 100\% \quad (3)$$

**For major (10-1/-101) face:** Referring to equation (3) and Figure S3 (a), with the measured thickness ( $t$ ) of the INDM crystal being **0.0043 mm** and Radius  $2R$  is **0.138 mm**, the calculated elastic bending strain is determined to be **~3.11%**.

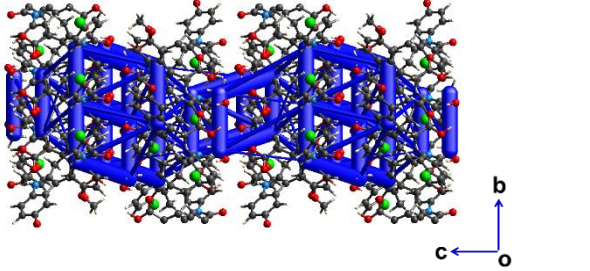
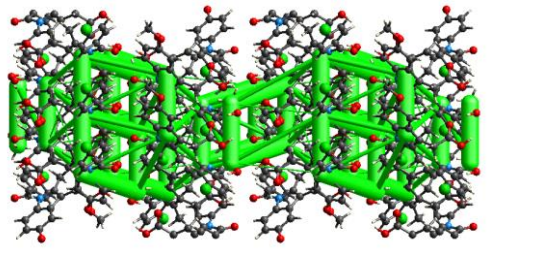
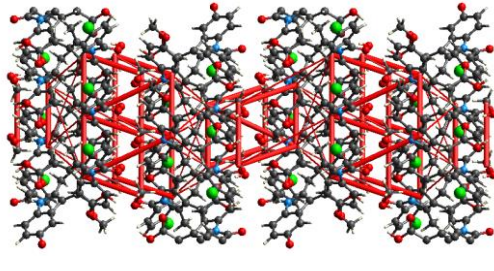
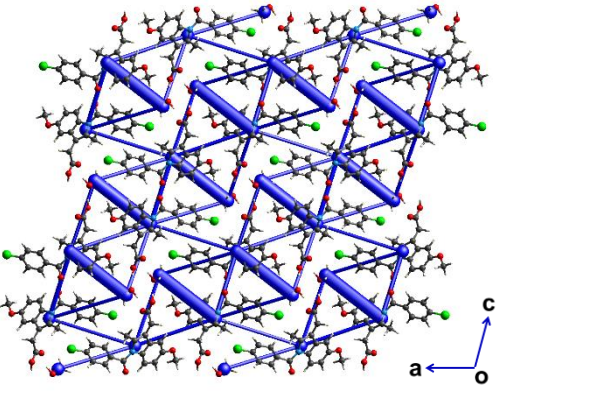
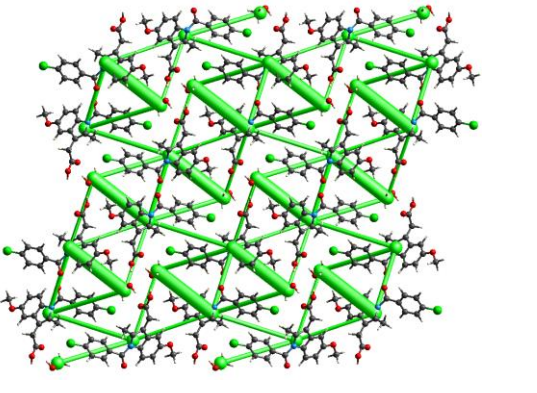
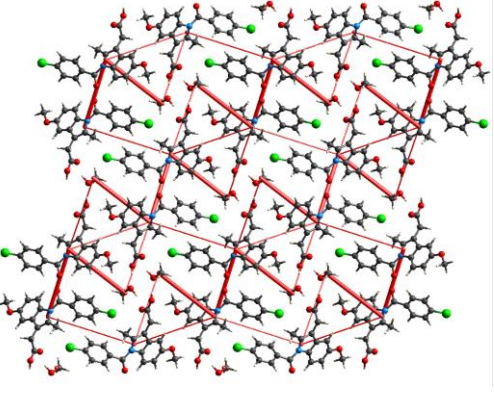
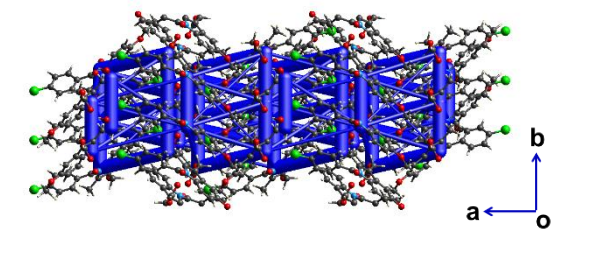
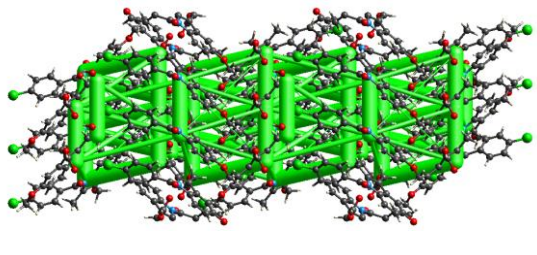
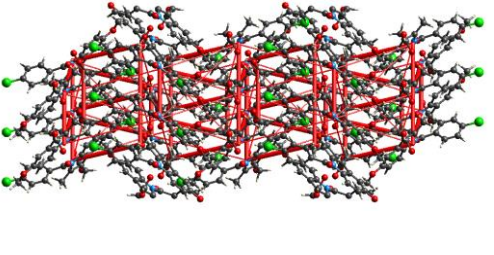
**For minor (101/-10-1) face:** Referring to equation (3) and Figure S3 (b), with the measured thickness ( $t$ ) of the INDM crystal being **0.017 mm** and Radius  $2R$  is **0.965 mm**, the calculated elastic bending strain is determined to be **~1.76%**



**Figure S3.** Maximum crystal elastic deformation of INDM (a) bending of (10-1)/(-101) plane, and (b) bending of (101)/(-10-1) plane.

### S6. Energy framework calculations.

Energy frameworks calculations for intermolecular interactions topologies for INDM were performed using the software suite Crystal-Explorer V.174 based on Gaussian B3LYP-D2/6-31G(d,p) molecular wave-functions calculated<sup>4</sup> using .cif of INDM, we collect the data from SCXRD (Table S1). The hydrogen positions normalized to standard neutron diffraction values for INDM molecules were used during the calculation. The interaction energies of a selected molecule with all molecules having any atom within  $3.8 \text{ \AA}$  were calculated. The interaction energies below a certain energy threshold ( $5 \text{ kJ/mol}$ ) were omitted for clarity, and the cylinder thickness was taken to be proportional to the intermolecular interaction energies in the energy framework.

Total Energy	Dispersion Energy	Coulomb Energy
		
a-axis	a-axis	a-axis
		
b-axis	b-axis	b-axis
		
c-axis	c-axis	c-axis

Interaction Energies (kJ/mol)

R is the distance between molecular centroids (mean atomic position) in Å.

Total energies, only reported for two benchmarked energy models, are the sum of the four energy components, scaled appropriately (see the scale factor table below)

	N	Symp	R	Electron Density	E_ele	E_pol	E_dis	E_rep	E_tot
	0	-x+1/2, y+1/2, -z+1/2	8.94	B3LYP/6-31G(d,p)	-6.7	-2.1	-29.5	26.4	-18.1
	0	x, y, z	4.99	B3LYP/6-31G(d,p)	-21.5	-6.3	-86.7	50.6	-71.6
	0	-x+1/2, y+1/2, -z+1/2	12.75	B3LYP/6-31G(d,p)	-5.1	-0.5	-6.9	0.0	-11.7
	0	-x+1/2, y+1/2, -z+1/2	10.62	B3LYP/6-31G(d,p)	-6.7	-2.6	-22.6	13.3	-20.5
	0	-x, -y, -z	7.62	B3LYP/6-31G(d,p)	-3.9	-4.2	-29.6	22.6	-19.1
	0	-	10.77	B3LYP/6-31G(d,p)	0.0	nan	0.0	0.0	nan
	1	-	8.02	B3LYP/6-31G(d,p)	-3.6	-0.5	-6.9	0.0	-10.1
	0	-	6.23	B3LYP/6-31G(d,p)	-0.2	-0.0	-0.2	0.0	-0.4
	0	-	8.37	B3LYP/6-31G(d,p)	-0.0	-0.1	-2.3	0.0	-2.1
	0	-	9.21	B3LYP/6-31G(d,p)	-6.7	-2.6	-22.6	13.3	-20.5
	0	-	6.25	B3LYP/6-31G(d,p)	0.3	-0.0	-0.7	0.0	-0.4
	0	-x, -y, -z	7.93	B3LYP/6-31G(d,p)	-20.9	-5.5	-20.3	29.9	-25.4
	0	-	8.41	B3LYP/6-31G(d,p)	-21.5	-6.3	-86.7	50.6	-71.6
	0	-	9.76	B3LYP/6-31G(d,p)	-3.9	-4.2	-29.6	22.6	-19.1
	0	-	11.58	B3LYP/6-31G(d,p)	-0.0	-0.0	-0.1	0.0	-0.1
	0	-	8.02	B3LYP/6-31G(d,p)	-0.6	-0.5	-6.9	0.0	-7.0
	0	-	6.23	B3LYP/6-31G(d,p)	-0.5	-0.0	-0.2	0.0	-0.7
	0	-	8.37	B3LYP/6-31G(d,p)	-0.0	-0.1	-2.3	0.0	-2.1
	0	-	8.41	B3LYP/6-31G(d,p)	-21.5	-6.3	-86.7	50.6	-71.6
	0	-	11.58	B3LYP/6-31G(d,p)	0.0	-0.0	-0.1	0.0	-0.0
	0	-	6.25	B3LYP/6-31G(d,p)	0.1	-0.0	-0.7	0.0	-0.6
	0	-x, -y, -z	4.68	B3LYP/6-31G(d,p)	0.0	-0.0	-0.0	0.0	0.0
	0	x, y, z	4.99	B3LYP/6-31G(d,p)	-21.5	-6.3	-86.7	50.6	-71.6
	0	-x, -y, -z	4.20	B3LYP/6-31G(d,p)	0.0	-0.0	-0.1	0.0	-0.0
	0	-	9.76	B3LYP/6-31G(d,p)	-3.9	-4.2	-29.6	22.6	-19.1
	0	-	10.77	B3LYP/6-31G(d,p)	0.0	nan	0.0	0.0	nan
	0	-	9.21	B3LYP/6-31G(d,p)	-6.7	-2.6	-22.6	13.3	-20.5

Scale factors for benchmarked energy models

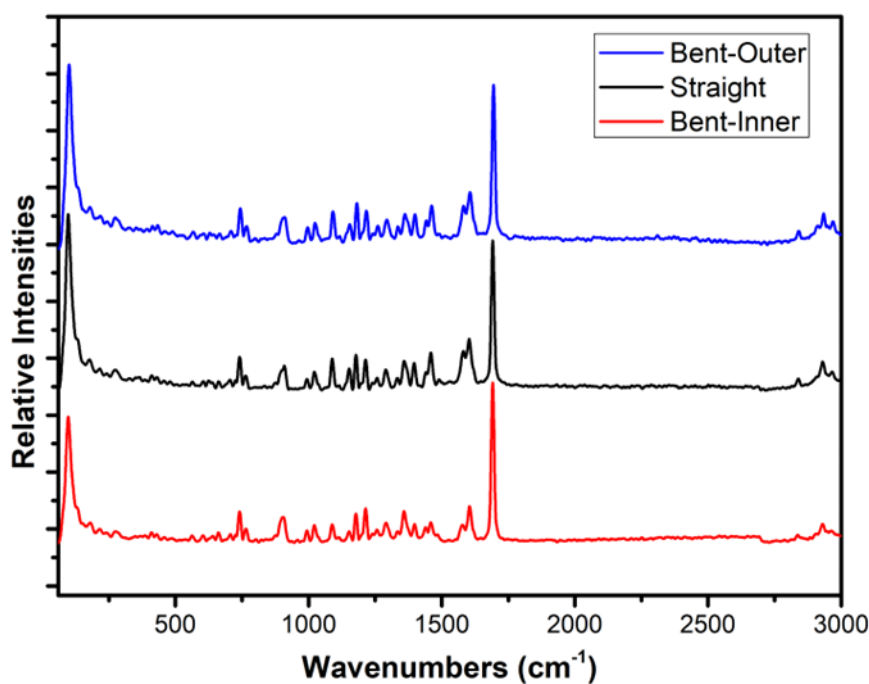
See Mackenzie et al. IUCrJ (2017)

Energy Model	k_ele	k_pol	k_disp	k_rep
CE-HF ... HF/3-21G electron densities	1.019	0.651	0.901	0.811
CE-B3LYP ... B3LYP/6-31G(d,p) electron densities	1.057	0.740	0.871	0.618

**Figure S4.** Energy framework calculation of INDM.

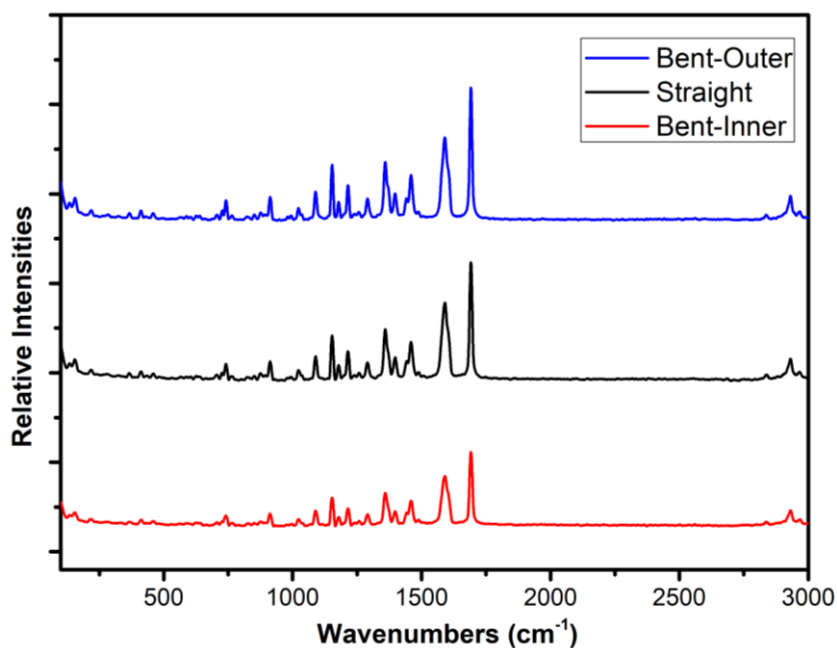
## S7. Raman Spectra of elastic INDM

Raman spectroscopy of bent crystals along two different faces (10-1)/(-101) and (101)/(-10-1) was prepared by attaching the two ends of a 2D elastic INDM crystal to a glass slide, thereby preventing it from returning to its normal straight state. Raman spectra of both straight and bent INDM crystals were recorded using a confocal Raman microscope (TechnoS IndiRAM CTR 500C Micro Raman Spectrometer, India) with a CCD detector (Fig. S5 and S6). A 532 nm diode laser was used to excite the INDM crystal samples. For the straight INDM crystal, a 50× lens was employed, and spectra were collected with an 8-second integration time and 5 accumulations. For the bent INDM crystal, spectra were acquired from both the inner and outer parts of the curve using the same 50× lens, which has a laser beam diameter of 1  $\mu\text{m}$ . For both inner and outer points on the bent crystal, the integration time was 8 seconds, and the average of 5 spectrum accumulations was recorded.



**Figure S5.** Full Raman spectra of straight and bent along (10-1)/(-101) face of INDM crystals.

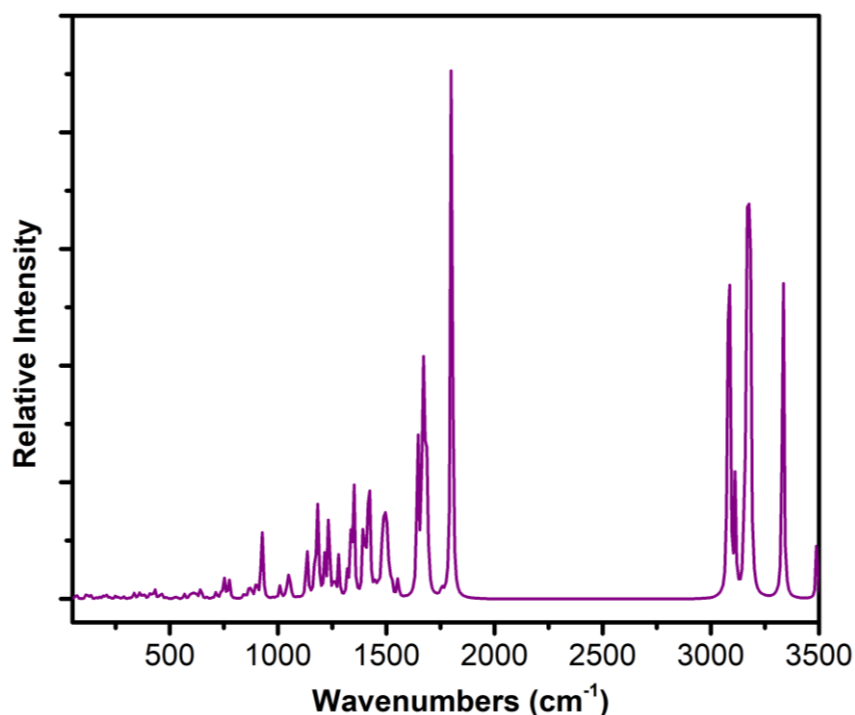




**Figure S6.** Full Raman spectra of straight and bent along (101)/(-10-1) face of INDM crystals.

### S8. Calculated Raman spectra of INDM

The vibrational computations of INDM were calculated by using Becke-3-Lee Yang Parr (B3LYP) density functional theory (DFT) method with 6-31G\*\* basis set in ground state using Gaussian-09 program to assign the relevant bands in the experimental spectra (Fig. S7).<sup>5</sup> The positive value of the calculated vibrational wavenumbers show that the optimized molecular structure is stable.



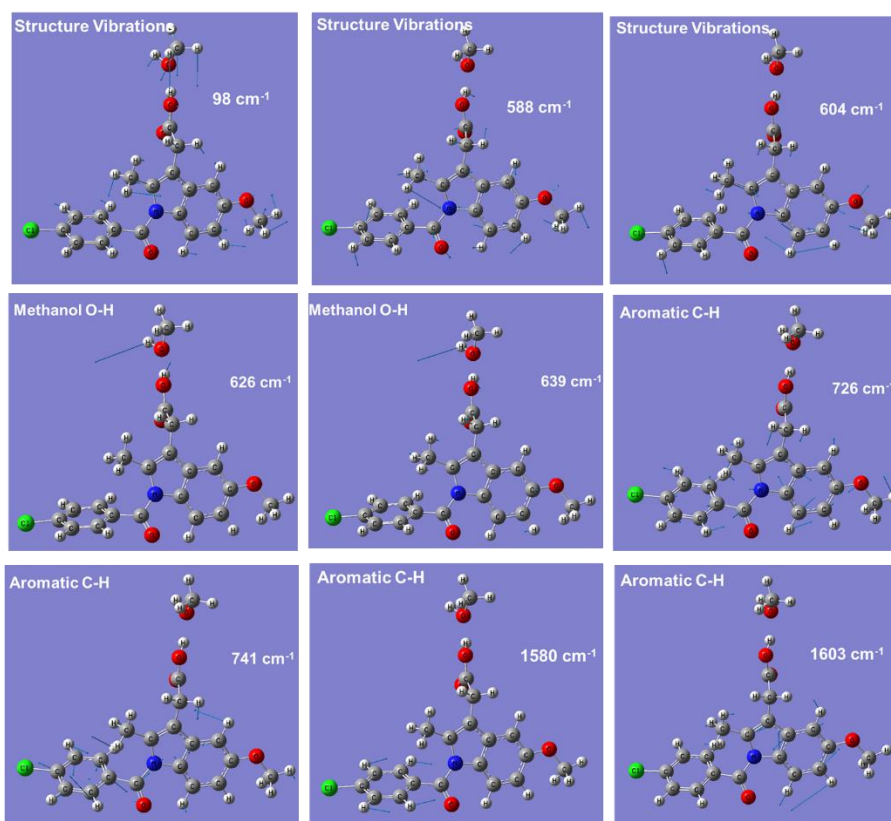


**Figure S7.** Calculated Raman spectra and selected peaks of INDM (top). Pictorial representation of vibrational modes (bottom).

### S9. SC-XRD frames before and after bending of INDM crystal

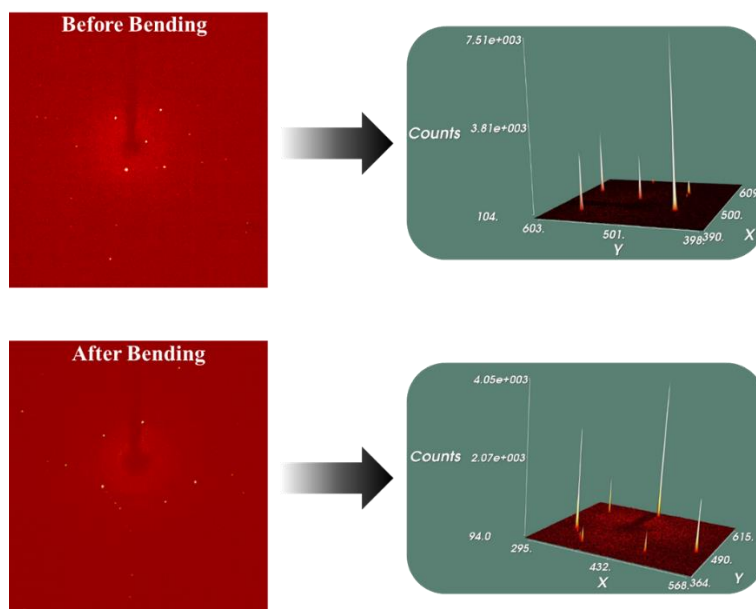


**Figure S8.** The SC-XRD frames indicate that the crystal quality of INDM crystals remained unchanged before and after bending.

## References:

1. J. G. Stowell, S. R. Byrn, G. Zografi, M. Yoshioka, CCDC 198477: Experimental Crystal Structure Determination. *CSD Communication* 2002 DOI: 10.5517/cc6njhv.
2. W. S. Rasband, ImageJ, U. S. National Institutes of Health, Bethesda, Maryland, USA, <https://imagej.nih.gov/ij/> (accessed Feb 13, 2019), 1997-2018.
3. S. P. Timoshenko, *History of Strength of Materials*; McGrawHill:New York, 1953.
4. M. J. Turner, J. J. McKinnon, S. K. Wolff, D. J. Grimwood, P. R. Spackman, D. Jayatilaka, M. A. Spackman, *CrystalExplorer17*. <http://hirshfeldsurface.net>.
5. M. J. Frisch, G. W. Trucks, H. B. Schlegel, G. E. Scuseria, M. A. Robb, J. R. Cheeseman, G. Scalmani, V. Barone, B. Mennucci, G. A. Petersson, H. Nakatsuji, M. Caricato, X. Li, H. P. Hratchian, A. F. Izmaylov, J. Bloino, G. Zheng, J. L. Sonnenberg, M. Hada, M. Ehara, K. Toyota, R. Fukuda, J. Hasegawa, M. Ishida, T. Nakajima, Y. Honda, O. Kitao, H. Nakai, T. Vreven, J. A. Jr. Montgomery, J. E. Peralta, F. Ogliaro, M. Bearpark, J. J. Heyd, E. Brothers, K. N. Kudin, V. N. Staroverov, R. Kobayashi, J. Normand, K. Raghavachari, A. Rendell, J. C. Burant, S. S. Iyengar, J. Tomasi, M. Cossi, N. Rega, J. M. Millam, M. Klene, J. E. Knox, J. B. Cross, V. Bakken, C. Adamo, J. Jaramillo, R. Gomperts, R. E. Stratmann, O. Yazyev, A. J. Austin, R. Cammi, C. Pomelli, J. W. Ochterski, R. L. Martin, K. Morokuma, V. G. Zakrzewski, G. A. Voth, P. Salvador, J. J. Dannenberg, S. Dapprich, A. D. Daniels, O. Farkas, J. B. Foresman, J. V. Ortiz, J. Cioslowski, D. J. Fox, *Gaussian 09*; Gaussian, Inc.: Wallingford, CT, 2009.